J. Cent. South Univ. (2014) 21: 2579−2583
DOI: 10.1007/s11771-014-2215-x

Springer

Fracture of thermal barrier coating with multiple surface cracks and delaminations: Interlayer effect

FAN Xue-ling(范学领)[1], XU Rong(许荣)[1], M. Kikuchi[2]

1. State Key Laboratory for Strength and Vibration of Mechanical Structures (School of Aerospace Engineering, Xi'an Jiaotong University), Xi'an 710049, China;
2. Department of Mechanical Engineering, Faculty of Science and Technology, Tokyo University of Science, Chiba 278-8510, Japan

Abstract: Multiple surface cracks and interfacial delamination are the major failure mechanisms in film/substrate systems. The effect of interlayer upon the failure mechanisms of interfacial delamination concomitant to surface crack was explored. Finite element model was developed to obtain the stress and energy release rate (ERR), which governs the propagation of interface cracks. The dependences of delamination upon the geometry and constitutive properties of interlayer were examined. The results indicate that the effect of elastic modulus of interlayer on the steady state ERR is insignificant. In cases of different geometrical parameters, however, the steady ERR decreases with the increase of the interlayer thickness. These findings lead to the conclusion that the interlayer constraint has significant effect on the ERR and thus coating life, which can be adopted to modify the ceramic top coat.

Key words: thermal barrier coating; delamination; interlayer; energy release rate

1 Introduction

Thermal barrier coating (TBC) is widely used to protect turbine and combustor engine components from the hot gas stream [1−3]. Current TBC system is usually composed of four layers, that is (1) the substrate, (2) the bond coat (BC), (3) the ceramic top coat (TC), and (4) the thermally grown oxide (TGO) formed during thermal cycling. The great difference in the thermo-mechanical properties of different layers makes the thermal-expansion mismatch stress become the most responsible factor for TBC failure [4]. In most studies of failure behavior of TBC, spallation has been emphasized with attention being given to thermal mismatch. In addition to being resistant to spallation from thermal cycling, a TBC on a gas turbine engine is also required to withstand damage from impact by hard particles of varying sizes [5−6]. According to the differences of size and velocity of particles, impact damage can lead to progressive loss of thickness (generally from smaller low-speed particles) or total spallation (from larger high-velocity particles). Therefore, except the desire of better spallation resistance from thermal cycling, greater impact resistance would also be desirable for more demanding applications at higher temperatures. Both of these two major failure modes are important issues which should be considered for advanced TBC design with enhanced reliability and thermal performance.

As pointed by BEGLEY and WADLEY [7], in comparison to studies of spallation and erosion mechanism in existing systems, relatively little attention has been directed at modifications to the ceramic TBC itself and associated fracture behaviors. Based on their experimental observations of a bi-layer coatings [8], the concept of ductile interlayer was proposed by ZHAO et al [9−10]. Their researches about the effects of thin plastically deformable interlayers on the lifetime of TBC have revealed that plastic straining in the ductile layers can lead to significant reductions in crack driving force by dissipating energy. The modification of top coat includes those performed by other researches [11−17]. They experimentally and numerically investigated the possibility of improving the durability of TBC by imparting vertical surface cracks into air plasma sprayed (APS) ceramic top coat. Experimental thermal cycling life of the modified TBC structures has resulted in the conclusion that appropriate preset surface cracks can increase the thermal strain tolerance of the coating, thus leading to the reduced crack driving force and less crack

Foundation item: Project(2013CB035700) supported by the National Basic Research Program of China; Projects(11272259, 11321062, 11002104) supported by the National Natural Science Foundation of China
Received date: 2013−06−15; **Accepted date:** 2013−12−02
Corresponding author: FAN Xue-ling; Tel: +86−29−82663318; E-mail: fanxueling@mail.xjtu.edu.cn

propagation at the top coat/bond coat interface. The pioneer work of the authors has contributed to our understanding of TBC structure design. As a result, based on our previous researches, a novel more durable multilayer TBC structure has been proposed [18], where vertical surface cracks are fabricated in the ceramic top coat to improve the durability of traditional APS TBC structure. The effect of periodic surface cracks on the interfacial fracture of TBC has been also investigated by FAN et al [19] using the finite element method incorporated with the cohesive zone model. Although considerable work has been done on the fracture mechanisms of the proposed TBC, it is not clear how an embedded interlayer affects the interfacial delamination of newly developed multilayer TBC structure. The goal of this work is to explore the effect of interlayer upon the fracture of surface crack and its concomitant interfacial delamination.

2 Statement of problem

As point out by HUTCHINSON and SUO [20], a steady state concept for cracks in multilayer structure is essential for many situations, where the crack driving force of channeling crack is independent of the tunnel length. As a result, the steady state crack driving force can be obtained by using a two-dimensional (2D) model.

A schematic illustration of the simplified 2D plane strain model of the analyzed TBC structure is shown in Fig. 1. An embedded interlayer is contained in the ceramic TC layer, where periodically vertical surface cracks and interfacial delaminations exist. As it has been illustrated, the Dundurs' parameters, α and β, can be used to characterize the elastic mismatch of the problem [20]. For the studied plane strain problem, the two nondimensional parameters can be expressed as

$$\alpha = \frac{\bar{E}_1 - \bar{E}_2}{\bar{E}_1 + \bar{E}_2} \tag{1}$$

$$\beta = \frac{1}{2}\frac{\mu_1(1-2\upsilon_2) - \mu_2(1-2\upsilon_1)}{\mu_1(1-\upsilon_2) + \mu_2(1-\upsilon_1)} \tag{2}$$

where $\bar{E}_i = E_i/(1-\upsilon_i^2)$, E_i, υ_i and μ_i (i=1, 2) are the plane strain modulus, elastic modulus, Poisson ratio, and shear modulus, respectively.

The traction on the interface ahead of the interface crack tip can be written as

$$\sigma_{yy}(x,0) + \mathrm{i}\sigma_{xy}(x,0) = K(2\pi r)^{-1/2} r^{\mathrm{i}\varepsilon} = (K_1 + \mathrm{i}K_2)(2\pi r)^{-1/2} r^{\mathrm{i}\varepsilon} \tag{3}$$

where $r^{\mathrm{i}\varepsilon}$=cos($\varepsilon$ln$r$)+isin($\varepsilon$ln$r$) represents the oscillatory singularity parameter for bimaterial interface crack problem, $\mathrm{i}=\sqrt{-1}$, and K corresponds to the complex stress intensity factor (SIF). The bimaterial constant has the form of

$$\varepsilon = \frac{1}{2\pi}\ln\frac{1-\beta}{1+\beta} \tag{4}$$

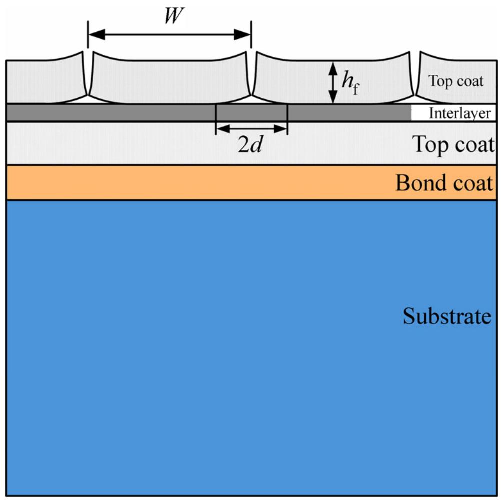

Fig. 1 Schematic illustration of an interlayered thermal barrier coating (TBC) structure

In finite element method (FEM), it is very convenience to calculate the J-integral around the crack tip, which makes it easier to obtain K according to Irwin's relationship between the energy release rate (ERR) and SIF.

Due to the periodicity of the analyzed problem, it is sufficient to consider a unit cell of the model with proper periodic boundary conditions. In this work, the technique modified by ZHANG et al [21] is employed on the left and right boundaries, which should remain parallel in a tangential sense. For simplicity, the TGO layer is assumed to have identical material properties as the bond coat. As a result, the complex TBC structure shown in Fig. 1 can be simplified to a four-layer representative unit cell model. To analyze the interfacial fracture more accurately, fine meshes are constructed around crack path. Four-node bilinear plane strain quadrilateral reduced integration elements are selected for all layers. The TBC is assumed to be subjected to a constant tensile traction through a uniform strain of 5%.

To further simplify the analysis, the ceramic TC layer as well as the BC and the substrate are assumed to be linearly elastic. The material properties of all layers are given in Table 1. The thicknesses for the TC, BC and substrate are chosen to be 200 μm, 100 μm, and 10 mm, respectively. Three interlayer thicknesses, 20 μm, 40 μm and 60 μm, are investigated in this work. For all studied cases, the width of the model (W) is assumed to be 4 mm. Except of the investigation on the influence of interlayer location, the distance from the center line of interlayer to TC/BC interface is kept constant of 100 μm.

Table 1 Material properties of thermal barrier coating (TBC) components

Component	Elastic modulus/GPa	Poisson ratio
Top coat	60	0.1
Interlayer	20, 60, 200	0.3
Bond coat	200	0.3
Substrate	211	0.3

3 Results and discussion

The SIF components are plotted in Fig. 2 as a function of normalized delamination length for different elastic moduli of a 60 μm interlayer, where $2d$ represents the delamination length. An intuitive conclusion can be driven that as the interface delamination propagates, a steady state is approached once a critical crack length is reached, which is comparable with the coating thickness. In the case of a stiff interlayer, by comparing Fig. 2(a) with Fig. 2(b), we can see that the dominant fracture mode is sliding (K_{II} is much larger than K_I). However, in contrast, much attention should be paid on the opening mode of a TC containing a relatively compliant interlayer. Since large mismatch stress, which usually leads to huge shear stress on the interface, will be induced in the coating upon cooling from the elevated temperature, a relative stiff interlayer is more severe for the thermal cycling life of TBC.

For interface crack problem, the mode mixity ψ, which is defined by $\psi=\tan^{-1}(K_{II}/K_I)$, is the measure of mode II to mode I loading acting on the interface crack. It is an important parameter to study interfacial fracture behavior of solids and structures. Figure 3 shows the variation of ψ as a function of the normalized interfacial debonding length for different interlayer elastic moduli. As delamination propagates, mode mixity reaches a steady state, which is intuitive in Fig. 3 since both of the SIF components approach constants for sufficient long delamination. The results further confirm the obvious difference of dominant fracture mode for relatively stiff and compliant interlayers.

Figure 4 shows the total ERR value as a function of normalized delamination length for the TBC containing a 60 μm interlayer. A strike feature in Fig. 4 is that compared with much difference in SIF components, the

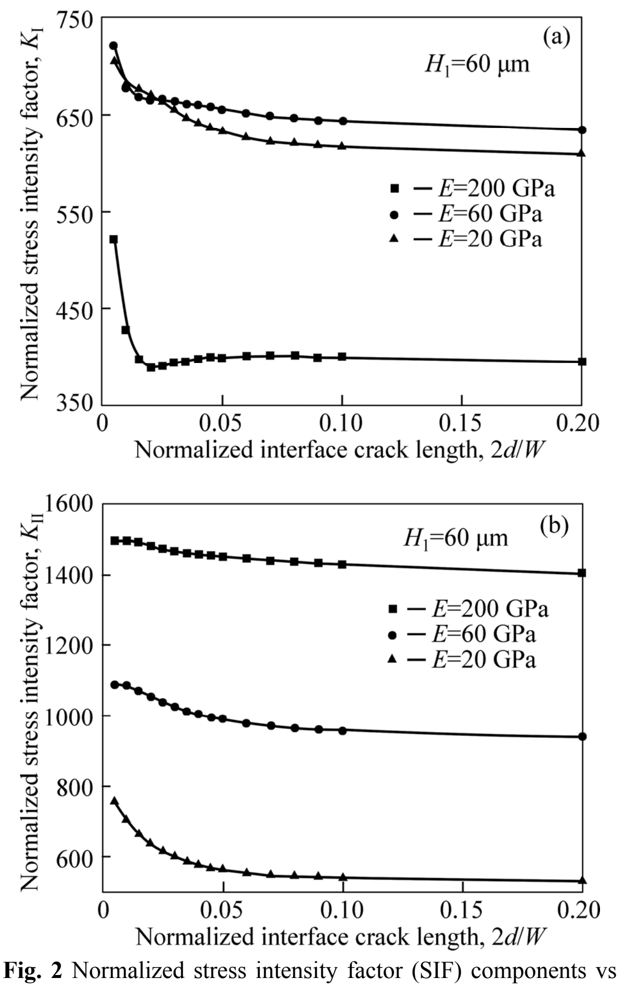

Fig. 2 Normalized stress intensity factor (SIF) components vs normalized interface crack length for different interlayer elastic moduli: (a) Mode I; (b) Mode II

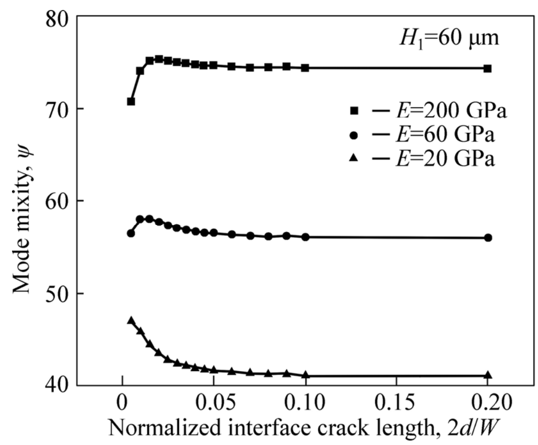

Fig. 3 Mode mixity vs normalized delamination length

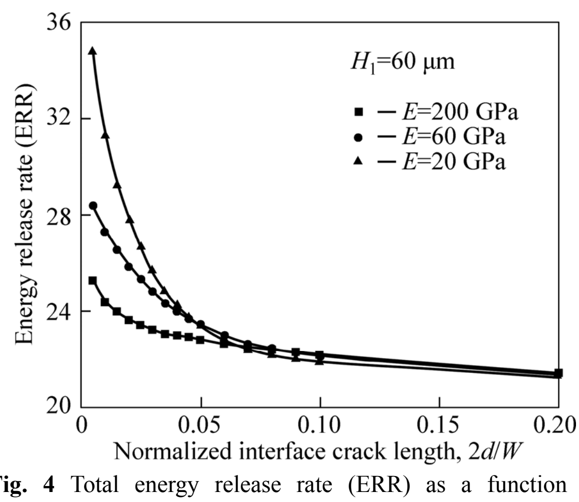

Fig. 4 Total energy release rate (ERR) as a function of normalized delamination length

ERR approaches a constant steady state value. We can conclude that the interlayer modulus has significant influence on the initiation of interfacial delamination while its effect can be ignored for relatively long delaminations. Based on the results, we are convinced that for practical TBC engineering applications, where the bonding strength is a material constant, the fracture mode will play the decisive role in the fracture of TBC.

Figure 5 shows the dependence of ERR on the interlayer thickness against delamination length. Similar behavior can be seen that steady state will be reached as delamination propagates. Any single line in Fig. 5 has the same interpretation as that in Fig. 4. One can note that with the extension of delamination, a same steady state will be reached for different elastic moduli of interlayer. However, different steady state ERR values are obtained in cases of various interlayer thicknesses. During the initiation process of interfacial delamination, the ERR decreases with the thickening of the interlayer, and rises with the decrease of the interlayer elastic modulus. After sufficient propagation, same trend is kept for cases of different interlayer thicknesses, which is quite different with the effect of constitutive parameter.

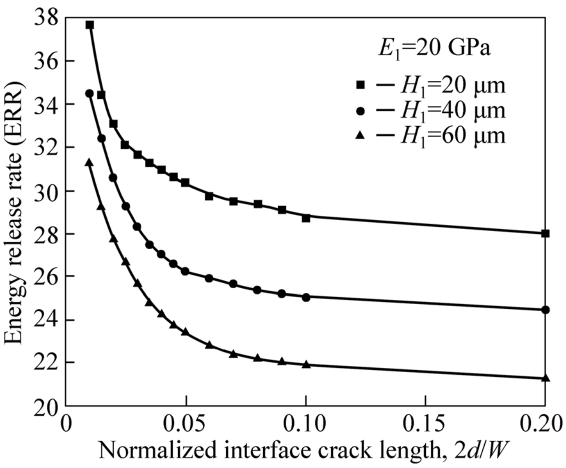

Fig. 5 Total ERR as a function of normalized delamination length

To explore the influence of interlayer location on the interface crack driving force, a parameter named “Offset” is defined in this work, which refers to the distance between the neutral axis of the interlayer and one imaginary line located 100 μm beneath the top surface. This parameter is used to illustrate the effect of relative position of the interlayer. From the results of Fig. 6, it is evident that as the interlayer moves to upper surface, the interface crack driving force is reduced. Therefore, it is advised that an interlayer with constant thickness should be kept far from the interface. Also, the effect of interlayer location seems more obvious than that of thickness and elastic modulus.

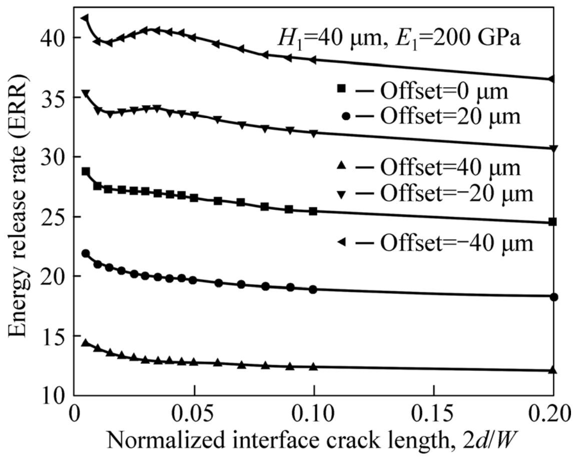

Fig. 6 Variation of ERR for different interlayer locations

4 Conclusions

1) It is indicated that with the extension of delamination, a constant steady state energy release rate (ERR) value is approached for different elastic moduli of interlayer. In contrast, significant difference of steady state ERR values exists for various interlayer thicknesses. The steady ERR value decreases as the interlayer thickness increases. To sum up, a thick, relatively compliant interlayer can lead to the reduction of interface crack driving force.

2) Future work will mainly cover the development of micromechanical models to explore the synergistic effects of embedded interlayer and the oxidation kinetics of bond coat and the impact resistance of the interlayer. Conducting a full thermal-mechanical analysis still requires the elasto-plastic constitutive model as well as the oxidation kinetics model which places the computational burden much higher than for ignoring the thickening of a thermally grown oxide.

References

[1] PADTURE N P, GELL M, JORDAN E H. Thermal barrier coatings for gas-turbine engine applications [J]. Science, 2002, 296(5566): 280−284.

[2] CLARKE D R, LEVI C G. Materials design for the next generation thermal barrier coatings [J]. Annual Review Materials Research, 2003, 33: 383−417.

[3] EVANS A G, CLARKE D R, LEVI C G. The influence of oxides on the performance of advanced gas turbines [J]. Journal of the European Ceramic Society, 2008, 28: 1405−1419.

[4] EVANS A G, MUMM D R, HUTCHINSON J W, MEIER G H, PETTIT F S. Mechanisms controlling the durability of thermal barrier coatings [J]. Progress in Materials Science, 2001, 46(5): 505−553.

[5] NICHOLLS J R, DEAKIN M J, RICKERBY D S. A comparison between the erosion behaviour of thermal spray and electron beam physical vapour deposition thermal barrier coatings [J]. Wear, 1999, 233/234/235: 352−361.

[6] CHEN X, HE M Y, SPITSBERG I, FLECK N A, HUTCHINSON J

W, EVANS A G. Mechanisms governing the high temperature erosion of thermal barrier coatings [J]. Wear, 2004, 256: 735−746.

[7] BEGLEY M R, WADLEY H N G. Delamination resistance of thermal barrier coatings containing embedded ductile layers [J]. Acta Materialia, 2012, 60: 2497−2508.

[8] BEGLEY M R, WADLEY H N G. Delamination of ceramic coatings with embedded metal layers [J]. Journal of the American Ceramic Society, 2011, 94(S1): S96−S103.

[9] ZHAO H B, BEGLEY M R, HEUER A, SHARGHI-MOSHTAGIN R, WADLEY H N G. Reaction, transformation and delamination of samarium zirconate thermal barrier coatings [J]. Surface & Coatings Technology, 2011, 205: 4355−4365.

[10] YU Z, ZHAO H B, WADLEY H N G. The vapor deposition and oxidation of platinum- and yttria-stabilized zirconia multilayers [J]. Journal of the European Ceramic Society, 2011, 94(8): 2671−2679.

[11] GUO H B, VAßEN R, STÖVER D. Atmospheric plasma sprayed thick thermal barrier coatings with high segmentation crack density [J]. Surface & Coatings Technology, 2004, 186: 353−63.

[12] ZHOU B, KOKINI K. Effect of pre-existing surface crack morphology on the interfacial thermal fracture of thermal barrier coatings: a numerical study [J]. Materials Science and Engineering A, 2003, 8(1/2): 271−279.

[13] ZHOU B, KOKINI K. Effect of surface pre-crack morphology on the fracture of thermal barrier coatings under thermal shock [J]. Acta materialia, 2004, 52(14): 4189−4197.

[14] THOULESS M D, LI Z, DOUVILLE N J, TAKAYAMA S. Periodic cracking of films supported on compliant substrates [J]. Journal of the Mechanics and Physics of Solids, 2011, 59: 1927−1937.

[15] FAN X L, ZHANG W X, WANG T J, LIU G W, ZHANG J H. Investigation on periodic cracking of elastic film/substrate system by the extended finite element method [J]. Applied Surface Science, 2011, 257(15): 6718−6724.

[16] ZHANG W X, FAN X L, WANG T J. The surface cracking behavior in air plasma sprayed thermal barrier coating system incorporating interface roughness effect [J]. Applied Surface Science, 2011, 258: 811−817.

[17] FAN X L, ZHANG W X, WANG T J, SUN Q. The effect of thermally grown oxide on multiple surface cracking in air plasma sprayed thermal barrier coating system [J]. Surface & Coatings Technology, 2012, 208: 7−13.

[18] WANG T J, FAN X L, ZHANG W X. A novel thermal barrier coating system [P]. China Patent, No.201110308546. 2012−04−25.

[19] FAN X L, XU R, ZHANG W X, WANG T J. Effect of periodic surface cracks on the interfacial fracture of thermal barrier coating system [J]. Applied Surface Science, 2012, 258: 9816−9823.

[20] HUTCHINSON J W, SUO Z. Mixed mode cracking in layered materials [J]. Advances in Applied Mechanics, 1992, 29: 63−191.

[21] ZHANG W X, WANG T J, LI L X. Numerical analysis of the transverse strengthening behavior of fiber- reinforced metal matrix composites [J]. Computational Materials Science, 2007, 39: 684−696.

(Edited by YANG Bing)